THE ASTROPHYSICAL JOURNAL, 440:210–215, 1995 February 10

NEW SYNTHETIC Mg_2 INDICES

M. CHAVEZ
International School for Advanced Studies (SISSA/ISAS), Strada Costiera 11, I-34014 Trieste, Italy; and
Instituto Nacional de Astrofisica, Optica y Electronica (INAOE), Mexico

M. L. MALAGNINI
Dipartimento di Astronomia, Università degli Studi di Trieste, Via Tiepolo 11, I-34131 Trieste, Italy

AND

C. MOROSSI
Osservatorio Astronomico di Trieste, Via Tiepolo 11, I-34131 Trieste, Italy
Received 1994 May 4; accepted 1994 August 26

ABSTRACT

Using the most recent grid of Kurucz model atmospheres and his improved set of numerical codes to compute synthetic stellar spectra, we have calculated the strength of the magnesium absorption feature at 5175 Å (Mg_2 index) from a set of 141 computed synthetic spectra. The index values refer to the effective temperature range 4000–6000 K, surface gravity from 1.5 to 4.5 dex, and metallicity from −0.5 to 1.0 dex. The computed index for the solar model matches very well the value obtained from observational data. Above 5000 K, the new Mg_2 values and previous calculations agree to within 0.02 mag, but discrepancies can reach almost 0.58 mag for cool, metal-rich, low-gravity stars, so that large values of Mg_2 previously obtained for low temperature dwarfs are now obtained for giants as well.

A comparison with observational data is also presented.

Subject headings: galaxies: photometry — galaxies: stellar content — stars: atmospheres

1. INTRODUCTION

In order to analyze the integrated light of stellar systems and its link to the basic parameters of a stellar population, it is fundamental to understand and to calibrate the behavior of the photometric and spectroscopic properties of the components (stars) in terms of the atmospheric stellar quantities, namely, temperature, gravity, and metallicity. These calibrations are coupled, in the context of the evolutionary synthesis, with a convenient set of evolutionary tracks to give insight into the overall changes of the radiation emitted by ensembles of stars with different characteristics. Once we know the dependence of the characteristics of the integrated radiation on all the free parameters involved, we should be able to determine the history and chemical evolution of stellar populations.

Empirical calibrations of several spectral indices (Faber et al. 1985; Buzzoni, Gariboldi, & Mantegazza 1992; Gorgas et al. 1993; Worthey et al. 1994, hereafter GW94) had led to a deeper understanding of their dependence on stellar atmospheric parameters.

Theoretical work initiated by Mould (1978) and continued by Gulati, Malagnini, & Morossi (1991, 1993, hereafter GMM93), Barbuy, Erdelyi-Mendes, & Milone (1992), McQuitty et al. (1994), and Barbuy (1994) has concentrated on a strong feature of magnesium at 5175 Å. In the following, we will refer to the Mg_2 index defined by Faber et al. (1985) mainly because of its potential in the analysis of integrated light of galaxies and because of the extensive set of observational data available (Gorgas et al. 1993; GW94).

The purpose of this paper is to present new synthetic Mg_2 indices, computed using the new set of Kurucz models (Kurucz 1993a) and codes to produce synthetic spectra (Kurucz 1993b, hereafter, with Kurucz 1993a, K93), and to compare them with already published indices (GMM93), based on previous Kurucz atmosphere models (1992, hereafter K92).

In § 2 we briefly describe the main differences between K92 and K93 grids of model atmospheres, atomic data, and codes. Section 3 is devoted to illustrating the relationships of the new set of Mg_2 indices to the atmospheric parameters, and the differences from the indices obtained by GMM93. In § 4, theoretical predictions are compared with empirical data, and conclusions are presented.

2. THE SYNTHETIC Mg_2 INDEX

GMM93 presented a grid of synthetic spectral indices based on a subset of the K92 grid of model atmospheres. This set of models included improvements with respect to previous versions and with respect to grids developed by other authors. These improvements were mainly the extension to a larger effective temperature range (from 50,000 K down to 3500 K), an increased set of atomic data in the opacity distribution functions, and, very important, the inclusion of opacity of diatomic molecules. GMM93 results showed that, for the case of the Mg_2 index, agreement within the observational errors is obtained when comparing synthetic indices with Gorgas et al. (1993) empirical calibrations, and with solar data.

The newest grid of Kurucz models (K93) contains a number of improvements and changes with respect to K92 models. Let us enumerate some of the principal changes (Kurucz 1994):

1. The new models contain 72 depth points starting at Rosseland optical depth 10^{-7} instead of 64 starting at 10^{-6}. This improvement removes the abrupt temperature drop at the surface that appeared in the earlier models, reduces the molecular abundances near the surface, and decreases the central depth of strong lines.

2. A bug in the Fe I continuous opacity at low temperatures was present in both the model atmosphere and spectrum synthesis programs. In K93 the bug was corrected.

3. A new SYNTHE series of programs to compute synthetic spectra includes a detailed treatment of scattering in the source function by default; in previous versions the default was a fast approximation based on the assumption of a small scattering fraction that led to trouble if applied where scattering is large.

The iron bug would produce an error that correlates both with temperature and with abundances. For instance, the temperature drop at the surface in the 64-depth model of the low-temperature giant star Arcturus affected the molecular number densities, and some of the molecular lines became weaker in the 72-depth model because the number densities decreased. This effect and the scattering change must be important in some cases.

We have used K93 models and codes to compute 141 synthetic stellar spectra. They refer to nine values of effective temperature in the range 4000–6000 K, surface gravities 1.5, 3.0, and 4.5 dex for metallicities −0.50, 0.5, and 1.0 dex, and log g from 1.5 to 4.5, with a step of 0.5 dex, for [M/H] = 0.0.

The solar metal abundances are from Anders & Grevesse (1989), and helium abundance is fixed at 10% by number. For nonsolar metallicities, the abundance of any element is scaled by the same ratio as [M/H]. The ratio of mixing length to scale height $l/h = 1.25$ is used for the treatment of convection (for more details, see K92).

The main computational characteristics of the synthetic spectra are the following:

1. microturbulence velocity $\xi = 2\ \mathrm{km\ s^{-1}}$;
2. resolving power $(\lambda/\Delta\lambda) = 250{,}000$;
3. rotational velocity of $0\ \mathrm{km\ s^{-1}}$.

In computing the synthetic Mg_2 indices, we adopted the definition of Faber et al. (1985; see Table 1 of GMM93) and used different values of the Gaussian broadening function (FWHM) to convolve the synthetic spectra. In what follows, we refer only to FWHM = 9 Å, in order to compare our results with those of GMM93 (Table 4) and with empirical data collected in the GW94 catalog.

3. RESULTS AND COMPARISON WITH GMM93

Table 1, and Figures 1 and 2, report the results obtained so far. The reliability of the new indices for temperatures in the range 5000–6000 K is confirmed by the result reported in Table 1 for the Sun. The synthetic Mg_2 value, computed starting from the solar model given in CD-Rom 18 (K93), matches very well that obtained from the solar observational data. The solar empirical index is derived from the high-resolution Fourier transform spectrometer (FTS) solar spectrum observed at the Kitt Peak Observatory (Kurucz et al. 1984), provided by Kurucz in computer-readable form. The index is computed by using the same procedure applied to any synthetic spectrum, according to the definition by Faber et al. (1985). Because of the high resolution of the spectrum (resolving power $\lambda/\Delta\lambda = 522{,}000$) and high signal-to-noise ratio (2000–9000), negligible photometric error, if any, is expected (errors lower than 1% in the residual flux are reported).

TABLE 1

Mg_2 INDEX FOR THE SUN (in magnitudes)

	Synthetic	
Observed	GMM93	This Work
0.135......	0.145	0.135

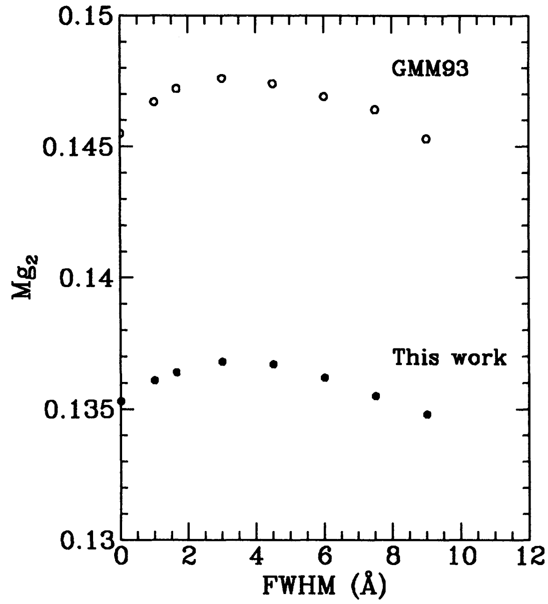

FIG. 1.—Dependence of the index on the FWHM of the Gaussian profile used in the convolution of the solar synthetic spectrum. Empty and filled symbols represent values from GMM93 and those obtained in this work, respectively.

Uncertainties in the computed solar index are estimated on the order of 0.005 mag when using different solar models in computing synthetic spectra. These uncertainties, as well as the difference between the synthetic GMM93 index and the empirical solar value, are on the same order as the expected errors for stellar observations.

The dependence of the index on instrumental resolution is displayed in Figure 1, with reference to the solar indices (empty circles correspond to the values given by GMM93, and filled ones to our results). Note that the trend is the same for both sets of data, with the new values located ~0.01 mag below, and that variations with FWHM of the broadening function are within a few thousandths of a magnitude.

Figure 2 contains three panels, where we plot new Mg_2 values versus the effective temperature parameter θ_{eff} ($\equiv 5040/T_{\mathrm{eff}}$). Each panel refers to one surface gravity value (1.5, 3.0, and 4.5 dex, respectively) and to four different metallicities; filled circles represent the indices computed for nine T_{eff} values, from 4000 K to 6000 K, at a step of 250 K.

The trend of the index with θ_{eff}, at fixed gravity, is quite similar when varying metallicity, while a clear difference is present at low temperature between giant and dwarf models. Indeed, for dwarfs a plateau is reached, while it is not for giants. In the panel referring to log g = 4.5 dex, the value computed for the solar model (5777/4.43770/0.00) is also plotted (*starred symbol*).

Figure 3 shows the comparison of GMM93 results with the present ones in 12 panels; each panel refers to one gravity and one metallicity (the difference for the Sun is marked as in Fig. 2).

The general trend of the differences between the two sets of data, illustrated in this figure, is the following: (1) new Mg_2 indices tend to be higher than in GMM93 at low temperatures

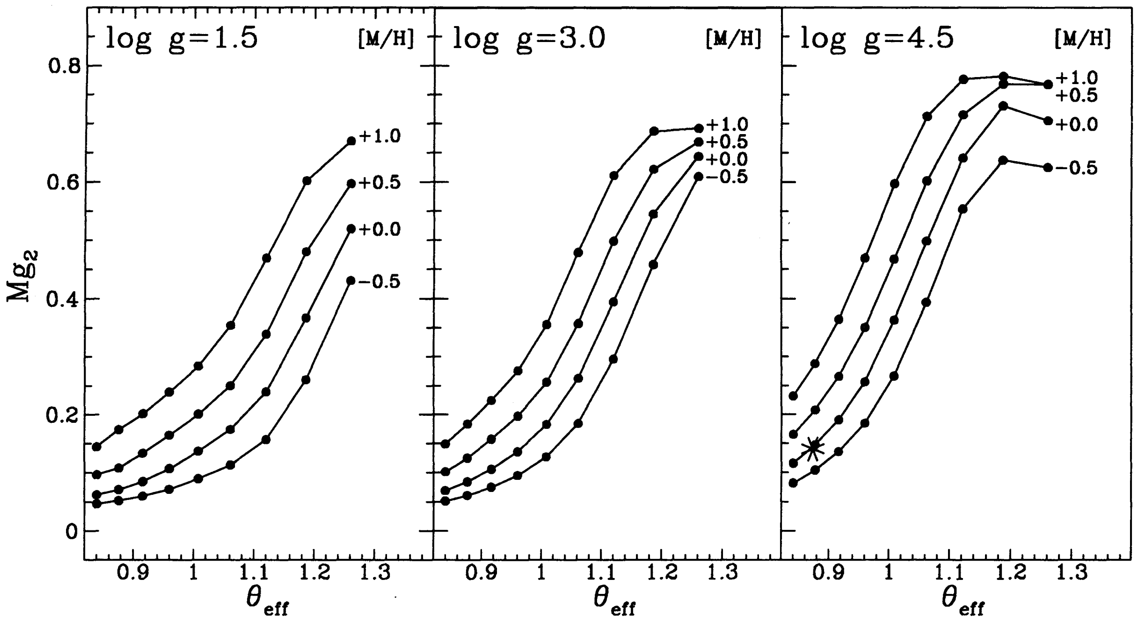

FIG. 2.—New synthetic indices for different metallicities and gravities as functions of θ_{eff}. The solar value is represented by a starred symbol.

and gravities, and at high metallicities; (2) the temperature above which old and new results do not differ significantly, irrespective of gravity, depends on metallicity. It goes from $T_{eff} = 4500$ K, for [M/H] = −0.5, up to 5250 K, for [M/H] = +1.0 dex.

In order to illustrate the effect of these differences in the interpretation of stellar data, we chose the case (4000/1.5), for which the differences are the highest The use of the new SYNTHE code starting from the same model as in GMM93 produced $Mg_2 = 0.5196$, to be compared with the new value ($Mg_2 = 0.5211$), and with the old one ($Mg_2 = 0.260$). We find that the differences in the models do not produce significant differences in the indices.

By comparing the new values for $T_{eff} = 4000$ K, log $g = 1.5$ dex, and different metallicities to the old ones, we find that new Mg_2 values are close to GMM93 ones reported for gravities higher than 1.5 dex: the difference in gravity goes from 0.75 dex for [M/H] = −0.5 up to 3.0 dex for [M/H] = 1.0. The net result is that Mg_2 values previously attributed to low-temperature dwarfs are now obtained for giants.

From these results and other tests, we conclude that the major differences in the indices are due to the different treatments of scattering in the codes, while only minor effects are due to differences in the models.

4. COMPARISON WITH OBSERVATIONAL DATA

To compare with observational data, we chose the most homogeneous collection of measured Mg_2 indices, presented by the Lick group (GW94) and kindly made available to us in a computer-readable form by the authors.

To establish the link between theoretical predictions and empirical data, the knowledge of atmospheric parameters, which naturally label the synthetic values, is required for the stars. We chose the most complete collection of (θ_{eff}, log g, [Fe/H]), with [Fe/H] derived from high-resolution analysis, i.e., A Catalogue of [Fe/H] Determinations: 1991 Edition (Cayrel de Strobel et al. 1992, hereafter C91). In the models, all metals are scaled by the same factor, thus the observed [Fe/H] values correspond to the theoretical [M/H] values.

The cross-check of the stars present in GW94 and of the determinations given in C91 produced a list of 501 entries. Out of this set, we extracted the determinations falling in the parameter ranges of our grid, leading to a final list of 141 determinations, referring to 67 stars.

The C91 atmospheric parameters were used to obtain synthetic Mg_2 indices from our grid by interpolating linearly in the three-dimensional space (θ_{eff}, log g, [M/H]). Table 2 contains, for the 67 stars present in C91 and GW94 in order of HD number, the atmospheric parameter determinations from C91, the observed indices from GW94, and the computed ones. The table is available in computer-readable form from M. L. M. (malagnini@univ.trieste.it).

The comparison between observed and synthetic indices is illustrated in Figure 4, where synthetic values from different determinations for the same star are connected by vertical bars.

In general, the points cluster around the 45° line, but it is clear that a large spread is present. The amplitude of the spread is much larger not only than the observational errors but also than the uncertainties expected in the synthetic values. By looking at different determinations for the same star, we can attribute most of the spread to uncertainties in the atmospheric parameters. This effect strongly affects the reliability of any empirical Mg_2 calibration based on heterogeneous and/or non–statistically unbiased data sets.

From Table 2 it results that the mean of the calculated indices is 0.03 mag (or 0.02 mag, if the two cool dwarfs with Mg_2[obs] > 0.4 mag—namely, HD 88230 and HD 219134—are excluded) larger than the mean of the observed values. This result is due to some extent to the use of linear interpolation for computing the synthetic values, while detailed investigation on individual stars with Mg_2(obs) > 0.4 mag is required to

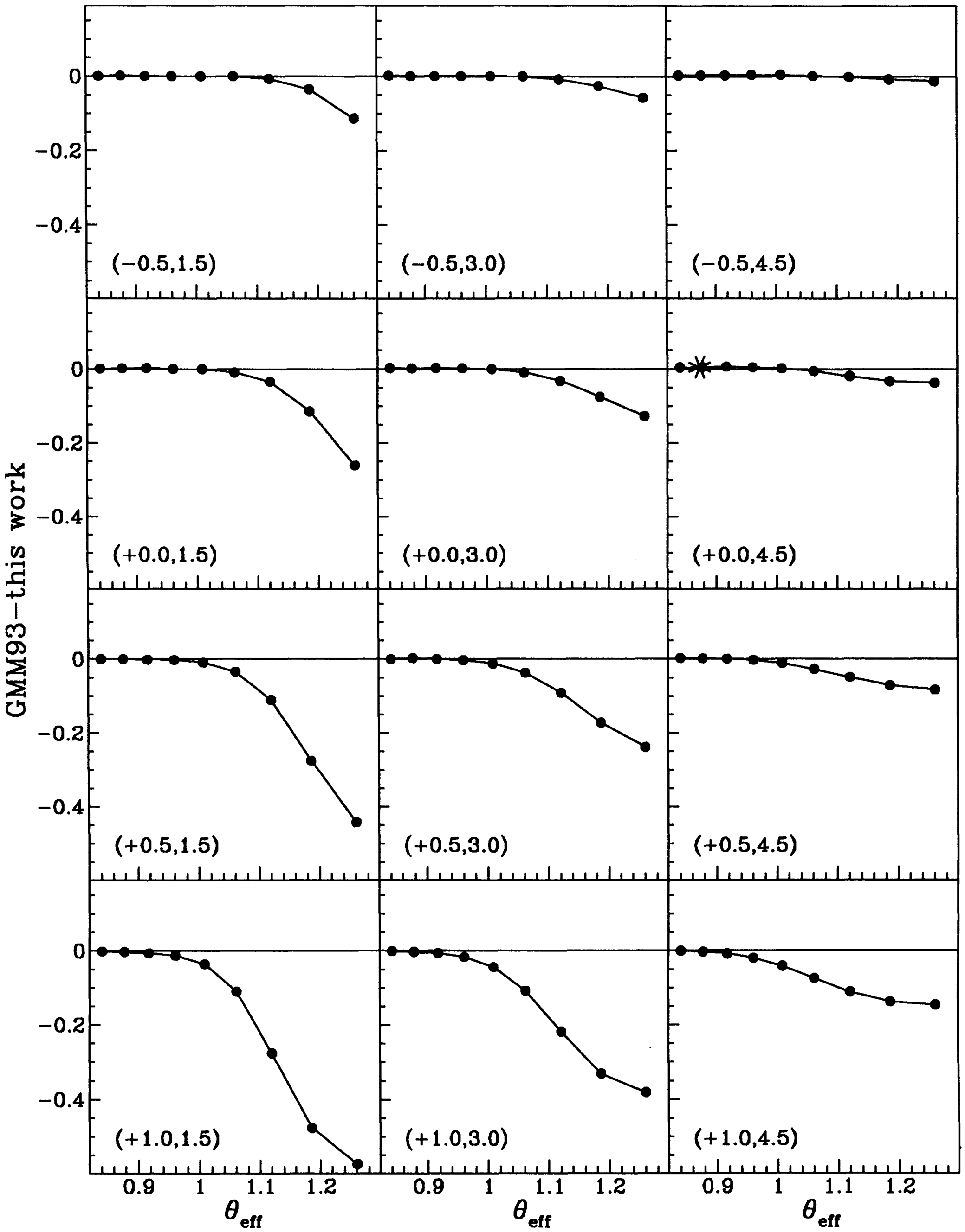

FIG. 3.—Differences between GMM93 and new synthetic indices for different metallicities and gravities as functions of $\theta_{\rm eff}$. The values of [M/H] and log g are given in parentheses in each panel. The solar case is represented by a starred symbol.

confirm the trend shown in Figure 4 by HD 88230 and HD 219134.

The absence in the observational database of cool dwarfs with atmospheric parameters from high resolution, prevents us from reaching any conclusive statement on the presence and level of any saturation in the index values (see discussion in Buzzoni et al. 1992).

In conclusion, the K93 release is expected to provide the best basis for stellar population studies, as its predictions are very closely confirmed by solar observations in different spectral regions, but comparisons with empirical spectral indices still present open problems, mainly because of insufficient accuracy in the determinations of stellar atmospheric parameters.

In the future we plan to produce extensive grids of Mg_2 and other spectral indices, covering the complete K93 metallicity range.

1995ApJ...440..210C

TABLE 2

ATMOSPHERIC PARAMETERS AND Mg_2 INDICES

HD	θ_{eff}	log g	[Fe/H]	Mg_2(obs)	Mg_2(comp)
3651	0.98	4.40	-0.17	0.277	0.262
4307	0.89	3.93	-0.36	0.088	0.106
4614	0.89	4.37	-0.17	0.078	0.140
	0.88	4.40	-0.20		0.130
10307	0.87	4.38	-0.03	0.127	0.134
10380	1.26	1.50	-0.35	0.315	0.458
	1.26	1.50	-0.30		0.467
10476	0.97	4.50	-0.20	0.271	0.248
10700	0.95	4.33	-0.49	0.210	0.165
12929	1.12	2.40	-0.21	0.229	0.283
	1.14	2.50	-0.08		0.360
	1.07	2.51	-0.25		0.203
13974	0.90	4.50	-0.30	0.132	0.143
14802	0.85	4.40	0.00	0.097	0.120
19476	1.02	3.30	0.08	0.188	0.242
	1.02	3.30	0.08		0.242
	1.01	2.68	0.19		0.198
20630	0.89	4.45	0.08	0.135	0.170
	0.89	4.40	-0.01		0.156
	0.90	4.50	0.04		0.178
22484	0.85	3.87	-0.16	0.090	0.091
	0.84	3.96	-0.12		0.088
23249	1.03	3.36	-0.27	0.253	0.218
	1.02	3.83	-0.07		0.279
	1.02	3.80	-0.20		0.259
	0.95	3.95	0.05		0.206
26965	0.99	4.31	-0.34	0.307	0.245
34334	1.22	2.10	-0.39	0.340	0.433
	1.20	2.30	-0.25		0.439
34411	0.86	4.11	0.35	0.117	0.153
	0.86	4.30	0.06		0.131
	0.86	4.10	0.30		0.148
35620	1.20	1.50	-0.09	0.361	0.376
37160	1.13	2.40	-0.31	0.174	0.291
39587	0.84	4.44	-0.12	0.122	0.106
	0.85	4.50	-0.05		0.121
41636	1.06	1.70	-0.30	0.227	0.144
47205	1.02	3.08	0.07	0.279	0.218
55575	0.87	3.98	-0.44	0.088	0.090
69267	1.17	1.87	-0.21	0.343	0.333
72324	1.07	2.25	-0.20	0.149	0.193
75732	0.97	4.50	0.24	0.305	0.325
	0.97	4.40	0.11		0.289
	0.97	4.50	0.30		0.336
82328	0.87	3.50	0.01	0.066	0.102
85503	1.13	2.40	-0.01	0.327	0.337
	1.14	2.30	0.03		0.357

HD	θ_{eff}	log g	[Fe/H]	Mg_2(obs)	Mg_2(comp)
85503	1.14	2.30	-0.11	0.327	0.333
	1.11	2.35	0.48		0.405
	1.07	2.82	0.11		0.285
	1.11	2.30	0.35		0.370
	1.17	2.20	0.31		0.474
86728	0.88	4.12	-0.08	0.144	0.128
	0.87	4.40	0.03		0.141
	0.89	4.33	-0.11		0.143
88230	1.26	4.50	0.28	0.518	0.741
88284	0.99	3.12	0.09	0.195	0.187
89010	0.90	4.00	-0.03	0.118	0.139
95272	1.05	3.01	0.10	0.203	0.263
102870	0.84	4.30	0.29	0.090	0.136
113226	1.02	2.70	0.01	0.140	0.182
	1.02	2.70	-0.03		0.178
	1.02	2.70	0.02		0.184
	1.01	2.85	0.04		0.182
	1.01	3.00	-0.10		0.173
	1.02	2.70	-0.06		0.175
	1.01	2.60	0.00		0.163
	1.01	2.75	-0.02		0.169
	1.01	3.00	0.17		0.210
	1.00	2.70	-0.05		0.155
	0.95	3.22	0.21		0.172
	1.01	2.70	-0.08		0.161
	1.01	2.70	0.10		0.184
114710	0.85	4.47	0.27	0.105	0.152
	0.85	4.40	0.02		0.122
115617	0.90	4.00	-0.03	0.162	0.139
	0.90	4.50	-0.02		0.171
117176	0.92	3.75	-0.11	0.137	0.135
124897	1.18	1.73	-0.43	0.273	0.294
	1.20	2.00	-0.32		0.390
	1.19	1.70	-0.49		0.298
	1.16	1.50	-0.38		0.243
	1.15	1.97	-0.42		0.269
132345	1.15	2.30	-0.02	0.317	0.371
	1.15	2.30	0.03		0.380
135722	1.05	2.70	-0.50	0.147	0.160
136202	0.84	3.90	0.00	0.072	0.091
140573	1.11	2.50	0.23	0.272	0.361
	1.09	2.39	-0.07		0.251
	1.10	2.90	0.37		0.415
	1.10	2.00	0.17		0.281
142373	0.87	3.93	-0.29	0.078	0.099
	0.85	4.30	-0.45		0.087
	0.85	4.30	-0.43		0.088

HD	θ_{eff}	log g	[Fe/H]	Mg_2(obs)	Mg_2(comp)
142373	0.85	4.30	-0.40	0.078	0.090
	0.86	4.00	-0.45		0.085
143761	0.87	3.98	-0.17	0.116	0.108
145675	0.97	4.50	0.22	0.298	0.321
	0.97	4.40	0.18		0.303
	0.93	4.50	0.31		0.261
153210	1.10	2.30	0.07	0.263	0.286
	1.10	2.30	-0.06		0.262
161797	0.91	3.91	0.16	0.165	0.166
	0.93	4.10	0.30		0.228
	0.93	4.10	0.32		0.231
165908	0.84	4.20	-0.39	0.064	0.082
	0.85	4.17	-0.42		0.086
166620	1.04	4.50	-0.20	0.343	0.402
	1.04	4.40	-0.30		0.368
182572	0.89	4.26	0.50	0.184	0.213
	0.88	4.13	0.44		0.185
	0.89	4.00	0.21		0.161
184406	1.06	2.85	-0.05	0.346	0.238
	1.07	2.10	0.00		0.205
185144	0.98	4.40	-0.25	0.213	0.250
186408	0.85	4.30	0.00	0.133	0.116
186427	0.86	4.50	0.08	0.136	0.142
	0.87	4.40	0.00		0.137
188512	0.99	3.15	0.29	0.179	0.221
	0.96	3.79	-0.15		0.182
190360	0.90	4.07	0.26	0.199	0.181
192310	1.01	4.50	-0.04	0.302	0.357
	1.03	4.50	-0.11		0.395
	1.01	4.50	-0.08		0.349
	1.01	4.50	-0.09		0.347
196755	0.89	4.40	-0.05	0.114	0.152
198149	1.00	2.95	-0.12	0.198	0.159
	1.00	3.15	0.23		0.223
	1.06	3.00	-0.50		0.183
203344	1.11	2.00	-0.20	0.221	0.231
215648	0.84	4.10	-0.28	0.058	0.085
217476	0.92	1.50	0.10	0.129	0.097
217877	0.84	4.50	-0.10	0.087	0.109
219134	1.07	4.50	0.10	0.452	0.538
	1.08	4.50	0.00		0.543
	1.08	4.40	-0.21		0.485
	1.07	4.50	0.00		0.518
	1.07	4.50	-0.01		0.516
	1.07	4.50	0.20		0.559
221148	1.07	2.60	0.07	0.370	0.256
222368	0.85	4.00	-0.18	0.063	0.094

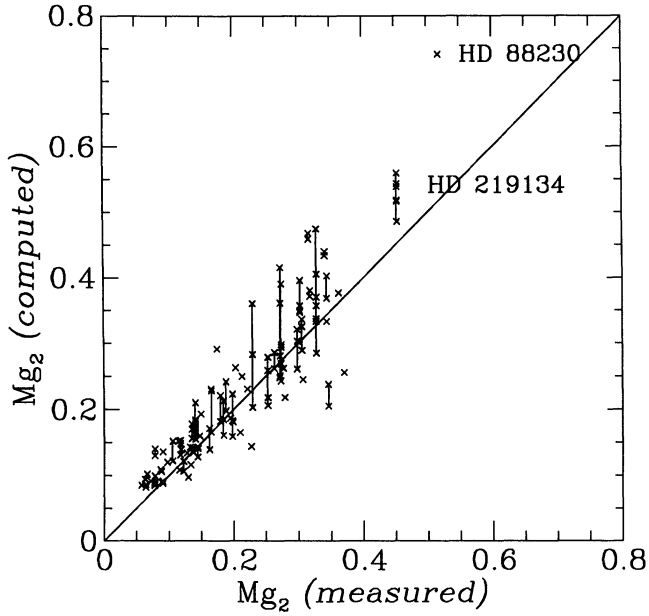

FIG. 4.—Plot of synthetic indices vs. the empirical values. Vertical bars connect the points referring to different determinations of atmospheric parameters given in C91 for the same star.

Further high-resolution analysis of cool stars, mainly late-type dwarfs and super–metal rich stars, is required to compare up-to-date theoretical predictions with empirical calibrations.

We thank G. Worthey for providing us with GW94 catalogue in computer-readable form and R. L. Kurucz and the referee for useful comments and suggestions. This work was partially supported by the Ministero dell'Università e della Ricerca Scientifica e Tecnologica (40% and 60% grants) and by the Consiglio Nazionale delle Ricerche (CNR-GNA and bilateral grants).

REFERENCES

Anders, E., & Grevesse, N. 1989, Geochim. Cosmochim. Acta, 53, 197
Barbuy, B. 1994, ApJ, 430, 218
Barbuy, B., Erdelyi-Mendes, M., & Milone, A. 1992, A&AS, 93, 235
Buzzoni, A., Gariboldi, G., & Mantegazza, L. 1992, AJ, 103, 1814
Cayrel de Strobel, G., Hauck, B., François, P., Thévenin, F., Friel, E., Mermilliod, M., & Borde, S. 1992, A&AS, 95, 273 (C91)
Faber, S. M., Friel, E. D., Burstein, D., & Gaskell, C. M. 1985, ApJS, 57, 711
Gorgas, J., Faber, S. M., Burstein, D., Gonzales, J. J., Courteau, S., & Prosser, C. 1993, ApJS, 86, 157
Gulati, R. K., Malagnini, M. L., & Morossi, C. 1991, A&A, 247, 447
———. 1993, ApJ, 413, 166 (GMM93)
Kurucz, R. L. 1992, in The Stellar Populations of Galaxies, ed. B. Barbuy & A. Renzini (Dordrecht: Kluwer), 225 (K92)
Kurucz, R. L. 1993a, CD-ROM 13, ATLAS9 Stellar Atmosphere Programs and 2 km/s Grid (Cambridge: Smithsonian Astrophys. Obs.)
———. 1993b, CD-ROM 18, SYNTHE Spectrum Synthesis Programs and Line Data (Cambridge: Smithsonian Astrophys. Obs.)
———. 1994, private communication
Kurucz, R. L., Furenlid, I., Brault, J., & Testerman, L. 1984, Solar Flux Atlas from 296 to 1300 nm (Sunspot: Nat. Solar Obs.)
McQuitty, R. J., Jaffe, T. R., Friel, E. D., & Dalle Ore, C. M. 1994, AJ, 107, 359
Mould, J. 1978, ApJ, 220, 434
Worthey, G., Faber, S. M., Gonzalez, J. J., & Burstein, D. 1994, ApJS, 94, 687 (GW94)